PERFORMANCE OF THE PBL PARAMETERIZATIONS IN THE GLAS AND UCLA MODELS

David A. Randall

Goddard Laboratory for Atmospheric Sciences
NASA/Goddard Space Flight Center
Greenbelt, MD 20771

1. INTRODUCTION

The planetary boundary layer (PBL) is the layer adjacent to the earth's surface within which vertical turbulent transports play a dominant role in the budgets of momentum, moisture, and sensible heat, and the turbulence energy is more-or-less continuously distributed in space and time.

In the early years of general circulation modeling, the PBL was recognized as an important dissipative mechanism (Charney and Eliassen, 1949), and as a significant regulator of the surface fluxes of sensible heat and moisture (Smagorinsky et al., 1965). Meanwhile, pioneering observational studies revealed the intimate coupling between the tropical PBL and the cumulus layer above (Bunker et al., 1949; Malkus, 1957), and the crucial role of tropical cumulus convection in the global energy cycle (Riehl and Malkus, 1958).

Then, during the 1960's and 70's, Lilly (1968) drew attention to the remarkably persistent marine subtropical PBL stratocumulus decks, and Herman and Goody (1976) described the similar PBL stratus layers of the Arctic summer. During these same years, much effort was devoted to understanding how the PBL turbulence is influenced by the variability of PBL depth, and the processes that produce that variability. Deardorff (1970; 1972; 1974a,b) showed that the PBL depth is determined by a rate equation in which turbulent entrainment plays a leading role, and that the stability dependence of the surface transfer coefficients can be expressed in terms of a bulk Richardson number which is proportional to the PBL depth. Arakawa and Schubert (1974) argued that the PBL depth tends to be reduced by the action of cumulus cloud ensembles, which

carry PBL mass up into the cumulus layer. They also pointed out that a deep PBL is favorable for cumulus activity.

As a result of these studies, the PBL is now understood to be much more than a near-surface layer of strong turbulent transports and kinetic energy dissipation. It serves as a variable-depth reservoir of moist air, and as a regulator for the tropical and mid-latitude-summer cumulus layers. Elsewhere on the globe, it harbors extensive and long-lasting stratocumulus layers, which are important features of the climate in their own right, and which dominate the radiation balance where they occur.

It is natural that some of the most important PBL processes are cloud-related. A large portion of the solar energy absorbed by the earth is introduced into the atmosphere through surface evaporation, in the form of latent heat. Because the PBL controls the evaporation and turbulent redistribution of water substance into the atmosphere, it strongly determines the global distributions of both cumuliform and statiform clouds. The clouds, in turn, influence the mean structure and turbulence of the PBL through cloud-induced circulations, through the radiation field, and through precipitation. A comprehensive simulation of PBL processess for a numerical model of large-scale atmospheric circulations must therefore include a simulation of the interaction of PBL with clouds. This aspect of the PBL parameterization problem has an importance comparable to that of the determination of the turbulent fluxes.

The problem of PBL parameterization for global circulation models therefore goes far beyond the problem of parameterizing the turbulent fluxes. The structure and variable depth of the PBL must be recognized, not only to determine the stability and storage capacity of the PBL, but also in the design of cumulus parameterizations. At the same time, the effects of cumulus activity on the PBL must be taken into account. The observed PBL stratus layers must be reproduced in any comprehensive climate simulation, and their very powerful effects on the PBL turbulence must be parameterized.

Furthermore, it is not enough to develop a physically sophisticated (and correct) model of the PBL which allows calculation of the response of the PBL to a given state of the free atmosphere. We must also carefully simulate the feedback and control mechanisms which determine the evolution of the free atmosphere and the PBL as a coupled physical system. This is possible only through careful design of the mathematical coupling between the parameterized PBL processes and the predicted variables of the numerical model.

This paper describes and presents some results of two PBL parameterizations currently being used in global general circulation models. The first is the very straightforward GLAS parameterization, in which the PBL depth is not predicted, the interaction of the PBL turbulence with cumulus and stratocumulus clouds is not parameterized, and the coupling of the PBL parameterization with the other components of the GCM is indirect. The second is the more complex UCLA parameterization, which includes as basic features a predicted PBL depth, explicit coupling of the PBL turbulence with cumulus and stratocumulus clouds, and direct coupling of the PBL parameterization with the rest of the GCM. The two models share the same surface flux parameterization, although the input parameters for the surface flux calculation are determined differently. Comparison of the two PBL parameterizations and the results obtained with them can show to what extent the greater complexity of the UCLA parameterization is justified.

In the next Section we present the prognostic equations governing the bulk properties of the PBL, as a framework for further discussion of the two parameterizations.

2. THE BULK EQUATIONS

A gross description of the state of the PBL can be given in terms of its depth, and its vertically-averaged potential temperature, mixing ratio, and wind vector. We refer to these as the bulk properties of the PBL. In this Section, we discuss the prognostic equations which govern these bulk properties.

The primitive forms of the conservation laws for dry air, potential temperature, moisture, the zonal and meridional wind components, and the turbulence kinetic energy can be integrated through the depth of the PBL to give

$$\frac{1}{g}\left[\frac{\partial}{\partial t}\,\delta p_M + \nabla\cdot(\underset{\sim}{V}_M\,\delta p_M)\right] - (E - M_{B+}) = 0\,, \tag{2.1}$$

$$\frac{1}{g}\left[\frac{\partial}{\partial t}\,(\theta_M\,\delta p_M) + \nabla\cdot(\underset{\sim}{V}_M\,\delta p_M\,\theta_M)\right] - E\,\theta_{B+} + M_{B+}\,(\theta_{cu,B+} - \theta_{B+})$$

$$= (F_\theta)_S + \frac{\theta}{cpT}\,(R_S - R_{B+} + LC_M)\,, \tag{2.2}$$

$$\frac{1}{g}\left[\frac{\partial}{\partial t}\,(q+\ell)_M\,\delta p_M + \nabla\cdot\underset{\sim}{V}_M\delta p_M\,(q+\ell)_M\right] - E\,(q+\ell)_{B+} + M_{B+}\,(q+\ell)_{cu,B+} - (q+\ell)_{B+}$$

$$= (F_{q+\ell})_S + r_{B+} - r_S\,, \tag{2.3}$$

$$\frac{1}{g}\left[\frac{\partial}{\partial t}\,(u_M\,\delta p_M) + \nabla\cdot(\underset{\sim}{V}_M\,\delta p_M\,u_M)\right] - Eu_{B+} + M_{B+}\,(u_{cu,B+} - u_{B+})$$

$$= -\left(\partial z/\partial x\right)_{p,M} + \left(f + \frac{u_M\tan\varphi}{a}\right)v_M + (F_u)_S\,, \tag{2.4}$$

$$\frac{1}{g}\left[\frac{\partial}{\partial t}\,(v_M\,\delta p_M) + \nabla\cdot(\underset{\sim}{V}_M\,\delta p_M v_M)\right] - Ev_{B+} + M_{B+}\,(v_{cu,B+} - v_{B+})$$

$$= -\left(\partial z/\partial y\right)_{p,M} - \left(f + \frac{u_M\tan\varphi}{a}\right)u_M + (F_v)_S\,, \tag{2.5}$$

and

$$\frac{1}{g}\left[\frac{\partial}{\partial t}\,(e_M\,\delta p_M) + \nabla\cdot(\underset{\sim}{V}_M\,\delta p_M e_M)\right] + M_{B+}\,e_{cu,B+}$$

$$= B + S - \frac{1}{\rho g}\,\delta p_M\,D_M\,. \tag{2.6}$$

Here δp_M is the pressure-depth of the PBL; subscript M otherwise denotes a vertical mean through the PBL; E is the entrainment mass flux at the PBL top; M is the cumulus mass flux; subscript B+ denotes a value just above the PBL top; $F_{(\ )}$ denotes the vertical turbulent flux of ( ); R is the net upward radiation flux; L is the latent heat; C is the rate of condensation; subscript cu denotes a value inside cumulus clouds; q and l are the mixing ratios of vapor and

liquid, respectively; subscript p denotes a derivative along an isobaric surface; r is the moisture flux due to precipitation; f is the coriolis parameter; φ is latitude; a is the radius of the earth; e is the turbulence kinetic energy (TKE) density;

$$B \equiv \delta_{pM} (F_{sv}/p)_M \cdot K \tag{2.7}$$

is the rate of generation of TKE by the buoyancy force;

$$S \equiv \delta_{p_M} (\underset{\sim}{F}_V \cdot \partial \underset{\sim}{V}/\partial p)_M \tag{2.8}$$

is the rate of generation of TKE by shear; and D is the rate of dissipation of TKE. In (2.7), K is the ratio of the specific gas constant for air to the specific heat of air at constant pressure, and s_v is the virtual dry static energy. All other notation is conventional.

Eqs. (2.2 - 2.6) do not contain terms representing turbulent transport at level B+ because we define this level to be above the PBL top, where turbulence is negligible. For the same reason, the cumulus term of (2.6) does not involve e_{B+}.

We have neglected lateral eddy transports.

As shown by (2.1), the PBL depth changes as a result of lateral mass convergence or divergence, turbulent entrainment or detrainment at the PBL top, and the loss of PBL mass into cumulus updrafts (Fig. 1).

In the derivation of the TKE equation (2.6), we have neglected a term representing the vertical transport of TKE by internal gravity waves above the PBL. Kantha et al. (1977) have presented experimental evidence that under some conditions such wave energy transport can substantially reduce the rate of entrainment into a mixed layer. But the magnitude of the wave-transport term depends in a complicated way on both PBL processes and the refractive structure of the free atmosphere. We have neglected this term for simplicity.

The cumulus terms of (2.1 - 2.6) represent the effects of the loss of PBL mass into cumulus updrafts. We have assumed for simplicity that all cumulus clouds of an ensemble share the same cloud-base values of θ, $(q+\ell)$, u, v,

and e. We have also neglected the effects of cumulus downdrafts which might penetrate the PBL independently of the turbulent entrainment process. We now assume, following Arakawa and Schubert (1974), that the air rising into cumulus clouds has the bulk properties of the PBL, i.e.

$$(\quad)_{cu,B+} = (\quad)_{M}. \tag{2.9}$$

This implies that, for example, cumulus clouds decrease the moisture content of the PBL (i.e. the mass of PBL water vapor per unit area) without decreasing the mixing ratio of the PBL air.

The bulk equations (2.1 - 2.6) are prognostic. Each equation contains horizontal advection terms, representing grid-scale processes, and each contains entrainment and cumulus terms which must be parameterized. The surface flux terms of (2.2 - 2.5) must be parameterized, as well as the radiation terms of (2.2), the condensation terms of (2.2 - 2.3), and the precipitation terms of (2.3). The pressure-gradient, coriolis, and metric terms of (2.4 - 2.5) are explicitly computed in the large-scale dynamics routines of the GCM. Finally, the production and dissipation terms of (2.6) must be parameterized.

3. THE SURFACE FLUXES

The determination of the turbulent fluxes at the earth's surface is the most familiar and most widely discussed aspect of the PBL parameterization problem, and during recent years promising new theories have significantly improved our understanding in this area. No new theory of the surface fluxes is proposed in the present paper; instead, the method of Deardorff (1972) is adapted to our needs. Deardorff's theory is an early example of what are now called Ekman layer similarity theories, in that it relates the surface fluxes to the bulk properties of the PBL. Moss and Rosenthal (1975) have applied Deardorff's method to a diagnostic study of a tropical cyclone. They obtained drag coefficients which, they concluded, agreed well with those obtained in earlier angular momentum budget studies of tropical cyclones.

Deardorff used the Monin-Obukhov similarity theory, as formulated by Businger et al., (1971), to relate the temperature, moisture, and wind profiles in the surface layer to the surface fluxes. He then gave additional similarity laws for the part of the PBL which lies above the surface layer, and matched these to the Monin-Obukhov similarity laws. The resulting equations determine the surface fluxes as functions of the bulk stability of the PBL, and the ratio of total PBL depth to the surface roughness length. Explicit information about the surface layer variables is not needed.

Following Deardorff, we determine the surface fluxes of sensible heat, moisture, and momentum using

$$(F_s)_S = \rho_S u_* c_\theta (s_g - s_M) , \tag{3.1a}$$

$$(F_w)_S = \rho_S u_* c_\theta \beta (q^*_g - w_M) , \tag{3.1b}$$

and

$$u_* = c_u u_M . \tag{3.1c}$$

Here $u_* \equiv (|\underset{\sim}{F}_V|/\rho)_S^{1/2}$ is the surface friction velocity c_θ and c_u are transfer coefficients, β is a measure of ground wetness which ranges from zero for dry ground to one for soaked ground or water surface, and the subscript g denotes a ground value. The surface stress $-(\underset{\sim}{F}_V)_S$ is assumed to be parallel to the PBL mean wind. This assumption can be justified by noting that under unstable conditions the PBL momentum is nearly well-mixed, while under stable conditions the PBL is often so shallow that the PBL mean wind and the surface wind are nearly indistinguishable.

The surface transfer coefficients c_u and c_θ depend on $\delta z_M/z_o$, where δz_M is the PBL depth and z_o is the surface roughness length, and on the bulk Richardson number Ri_B, which is a bulk measure of the PBL's gravitational stability. The bulk Richardson number is defined in terms of the virtual dry static energy

$$\begin{aligned} s_v &\equiv c_p T (1 + 0.609q - \ell) + gz \\ &= s + c_p T (0.609q - \ell) . \end{aligned} \tag{3.2}$$

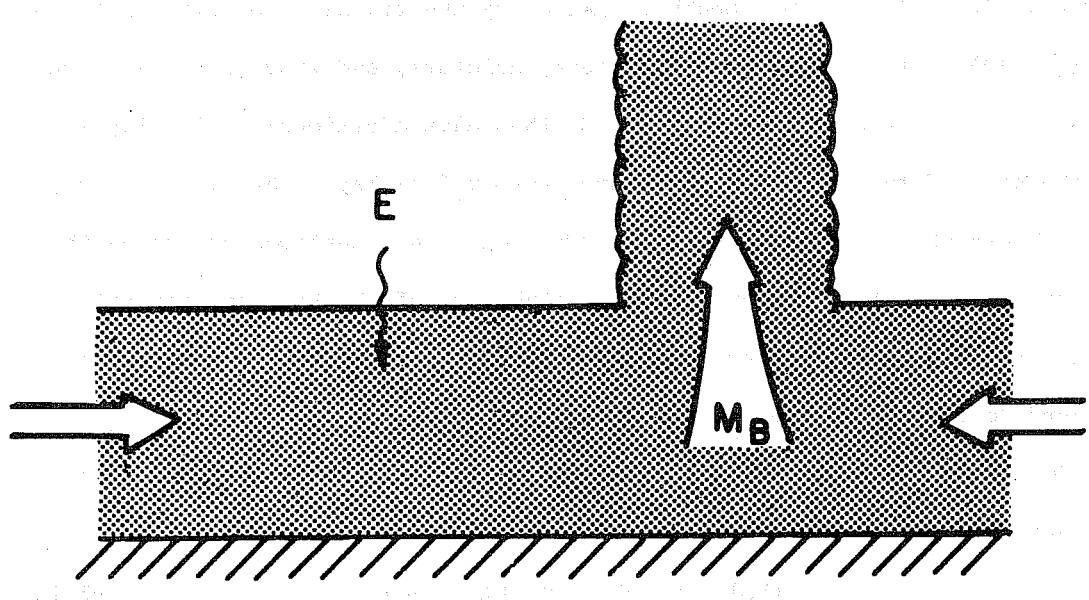

Figure 1. Diagram illustrating the mass budget of the PBL.

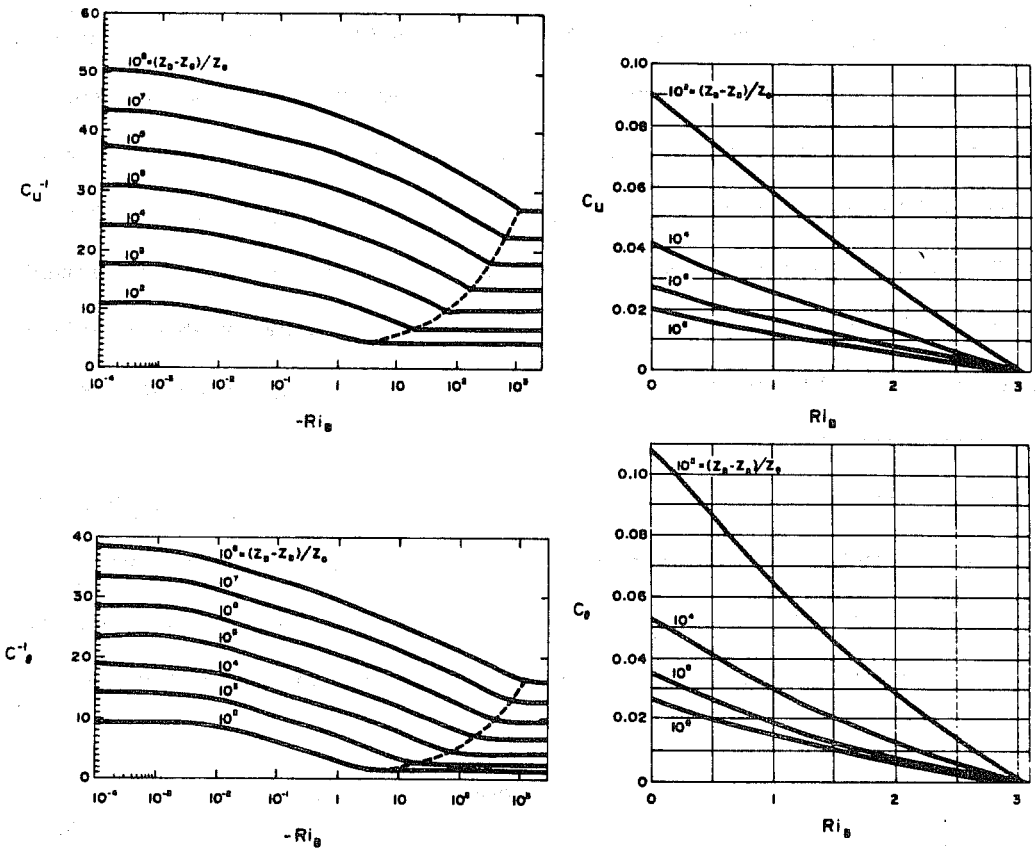

Figure 2. Dependence of the surface transfer coefficients on stability and surface roughness, after Deardorff (1972).

which is a measure of the relative buoyancy of air particles at the same level, taking into account the effects of both vapor and liquid. The bulk Richardson number is

$$Ri_B = \frac{-g \, \delta z_M \, (s_{vg} - s_{vM})_e}{c_p \, T_S |V_M|^2} \quad , \tag{3.3}$$

where $(s_{vg} - s_{vM})_e$ is the effective s_v difference between the ground and the air.

The functional dependence of c_θ and c_u on R_{iB} and $\delta z_M/z_0$ is shown in Figure 2, which is taken from Deardoff's paper. For further discussion, and for the equations represented in Figure 2, refer to Deardorff (1972).

For the purpose of computing the turbulent fluxes, the earth's surface is characterized by a temperature, a measure of surface wetness, and a roughness length. In both GCMs the ground temperature and wetness are predicted at land points (including prescribed sea ice points), and the sea surface temperature is interpolated daily from observed monthly climatological values. The surface roughness length is prescribed at all points, as shown in Table 1.

Terrain Type	Prescribed z_o, Meters	Reference
Land	0.45	Fiedler and Panofsky (1971)
Water Surface	2.0×10^{-4}	Fiedler and Panofsky (1971)
Sea Ice	1.0×10^{-4}	Ling and Untersteiner (1974)

Table 1. Surface roughness lengths used in both parameterizations.

In order to evaluate the surface fluxes we must determine the PBL mean wind vector, the bulk values of the virtual dry static energy and mixing ratio, and the PBL depth. These quantities are determined very differently in the GLAS and UCLA models, as explained in the following sections.

4. A DESCRIPTION OF THE GLAS PARAMETERIZATION

The nine-level GLAS climate model is descended from the 1970 version of the UCLA model. Descriptions of the model in various stages of development are given by Sommerville et al. (1974), Halem et al. (1979), and Shukla et al. (1982).

Until recently, the model's PBL parameterization was that developed by Katayama (described by Arakawa, 1972), as modified by Sommerville et al. (1974). It included stability dependence, but without the virtual temperature effect. The transfer coefficients for sensible heat, moisture, and momentum were assumed to be equal, and increased both with increasing wind speed over the ocean and with increasing surface height over land.

The model has recently been modified by Randall (1982) to make use of the surface flux parameterization described in Section 3. The bulk properties of the PBL, which are needed as input to the prameterization, are determined by the following very simple approach: The PBL depth is taken to be 500 m everywhere and at all times. This value has been chosen because it is near the observed depth of the marine trade wind PBL, which covers much of the planet, and because it represents a rough daily mean depth for the PBL over land. The bulk values of the virtual potential temperature, mixing ratio, and wind components are determined by a simple extrapolation in height from the lowest two GCM layers to the mid-level of the PBL, i.e. 250 m. No attempt is made to allow for the inversions and other sharp features which are sometimes observed at the PBL top.

The extrapolated virtual potential temperature and mixing ratio are not used to detect the presence of PBL stratocumulus clouds, since without a predicted PBL depth there is no way for the clouds to influence the evolution of

the PBL, and also because the radiation parameterization of the GCM is designed to deal only with clouds which fill the full vertical extent of a GCM layer.

The cumulus parameterization was developed by Sommerville et al. (1974) from that designed by Arakawa (1972) for the three-level UCLA GCM. A description of the parameterization is given by Helfand (1979). The lowest allowed cumulus cloud base level is at the top of the second model layer; obviously, this level is well above the PBL top.

5. RESULTS FROM THE GLAS GCM

We present results from a July simulation, initialized from the observed state of the atmosphere for June 15, 1979.

The recent introduction of the surface flux parameterization described in Section 3 has led to a dramatic improvement in the model's ability to simulate observed monthly-mean sea level pressure patterns. Fig. 3 shows the zonally-averaged sea level pressure according to observations, and as simulated by the current GLAS model, an earlier GLAS model which used the Katayama surface flux parameterization, and the UCLA model. The new GLAS model and the UCLA model, which share the same surface flux parameterization, both produce fairly deep low pressure belts over the ocean around Antarctica, and both simulate strong subtropical highs in the Southern Hemisphere. The earlier GLAS model fails to simulate the intensity of these features, and so fails to produce a belt of strong surface westerlies near 50°S. Although the surface flux parameterization is not the only difference between the "new" and "old" GLAS models, we believe it is the main reason for the improvement seen in Fig. 3. Further discussion is given by Randall (1982).

Fig. 4 shows the simulated July mean total cloudiness. The shaded areas are those in which the cloudiness is less than 70%. Although cloudiness maximum of the ITCZ and the cloudiness minima of the subtropics are qualitatively captured, a glaring deficiency apparent in the figure is that the cloudiness is excessive, at almost every latitude. The simulated planetary albedo is 0.40.

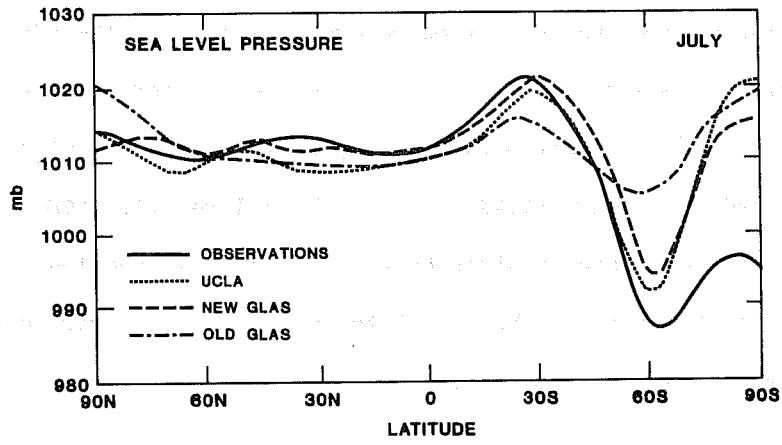

Figure 3. Zonally-averaged sea-level pressure.

Most of the excessive cloudiness is due to widespread supersaturation in the lowest model layer. (This deficiency of the model was evident both before and after the surface flux parameterization was revised.) The simulated evaporation and precipitation distributions are fairly realistic (Shukla et al., 1982) but the model does not properly transport the evaporated moisture up out of the bottom layer. We believe that there are two reasons for this. First, the PBL parameterization does not permit PBL moisture to be mixed upward into the free atmosphere through the diurnal variation of PBL depth over land. Second, the model's cumulus parameterization does not directly dry the PBL by lifting moisture in cumulus updrafts.

Fig. 4 also shows that the model fails to simulate the observed spectacular July cloudiness maxima off the west coasts of North and South America, and South Africa. In fact, the model actually simulates cloudiness minima in these regions, where large-scale subsidence associated with the subtropical highs naturally tends to produce dry low-level air. In nature, the moist and cool PBL is observed to contain extensive stratocumulus sheets, which account for the observed cloudiness maxima. As dry subsiding air is entrained into the PBL, it is very rapidly moistened by turbulent moisture transport from below (Randall, 1980b). The GLAS model incorporates no parameterization of this process, and so it cannot simulate the observed cloudiness maxima.

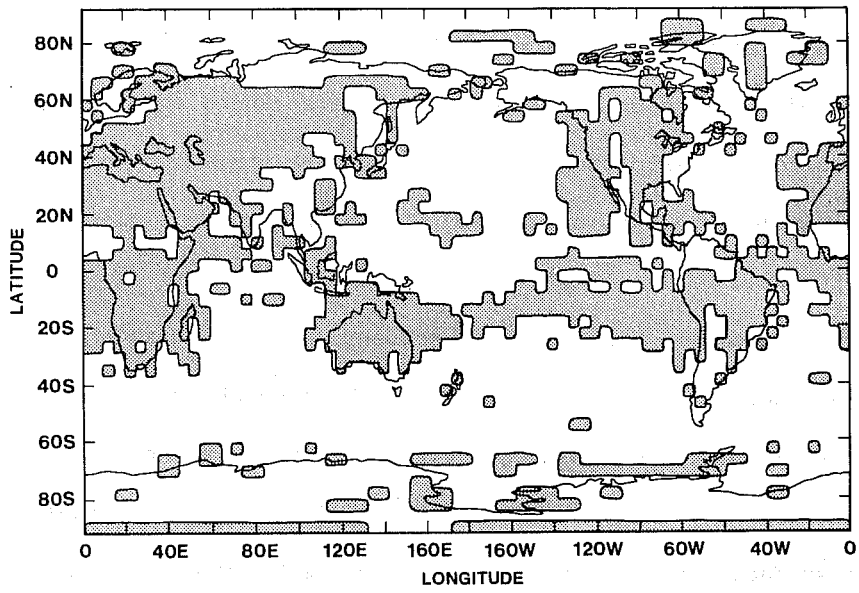

Figure 4. Total cloudiness simulated by the GLAS model. In the shaded regions the cloudiness is less than 70%

6. A DESCRIPTION OF THE UCLA PARAMETERIZATION

6.1 Coupling the PBL Parameterization with the Rest of the GCM

We shall present results from the 9-level tropospheric version of the UCLA GCM. A description of the finite-difference schemes of the model is given by Suarez and Arakawa (1979). The model includes the Arakawa-Schubert cumulus parameterization (Arakawa and Schubert, 1974; Lord and Arakawa, 1980; Lord, 1982; Lord, Chao, and Arakawa, 1982). Other results have been presented by Mechoso et al. (1979, 1981).

The PBL parameterization is incorporated into the GCM through the use of a generalized sigma-coordinate, in which the PBL top is a coordinate surface (Suarez and Arakawa, 1979). To explain the motivation for this choice, we review several alternatives which were considered and rejected as the PBL parameterization and the UCLA GCM evolved together over a period of years.

An early decision in the design of the PBL parameterization was that the PBL depth should be carried as a prognostic variable of the GCM. As discussed in the Introduction, observational and theoretical studies of the sixties and early seventies showed that the depth of the PBL is prognostically determined,

that it helps determine the bulk stability of the layer, and that it influences the level of cumulus activity. On a more elementary level, the depth of the PBL is a measure of how much of the lower troposphere can be modified by the surface fluxes, since by definition it is only the PBL air which is directly modified. For example, the rate of warming of the PBL due to a given surface sensible heat flux will be larger if the PBL is shallow than if it is deep, because the warming tends to reduce the subsequent surface sensible heat flux. This control loop exerts a powerful negative feedback on the surface sensible heat flux (and, analogously, on the other surface fluxes); a successful PBL parameterization must faithfully model the control loop. Fig. 5 schematically illustrates the surface flux control loops. Accurate knowledge of the PBL depth is essential for this purpose. Since the current PBL depth depends on its past history, a prognostic equation is required.

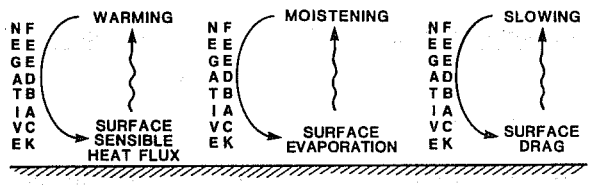

SURFACE FLUX CONTROL LOOPS

Figure 5. The surface flux control loops.

This conclusion leads directly to one of the most troublesome problems in the design of the PBL parameterization: How should a PBL of highly variable depth be incorporated into a vertically discrete GCM? On each timestep, it is necessary to determine, at the very least, the bulk potential temperature, mixing ratio, and wind vector for the PBL, in order to evaluate the surface fluxes, the entrainment rate, and the cumulus mass flux. These bulk variables satisfy the prognostic equations (2.2-2.5).

Deardorff (1972) suggested an extrapolation procedure in which the known PBL depth, GCM layer depths, and GCM layer properties are used to determine the bulk PBL properties. However, there are two difficulties with this approach.

First, as discussed by Deardorff, the PBL top is frequently observed to be marked by sharp jumps in the potential temperature and other quantities. At other times, the vertical derivative of the potential temperature is observed to change suddenly at the PBL top. Under these conditions, accurate extrapolation is not possible.

A second difficulty is that if the bulk properties are obtained by an extrapolation, the bulk prognostic equations (2.2-2.5) cannot be exactly satisfied. The prognostically determined PBL depth and the extrapolated bulk properties are used to determine the time rates of change of the GCM layer quantities and the PBL depth. These variables are time-stepped forward in the usual way. The extrapolation is then repeated, yielding new values of the bulk quantities and, implicitly, determining the time-rates-of-change of these quantities over the preceding time-step. In general, it is not possible to make these implicitly determined time-rates-of-change agree with those explicitly given by (2.2-2.5). This means that the control loops cannot be well-simulated.

In order to avoid this difficulty, it is necessary to introduce additional prognostic variables for the bulk structure of the PBL. However, if the bulk variables Θ_M, $(q + \ell)_M$, u_M, and v_M are predicted explicitly, new problems arise. Suppose, for example, that at a particular grid-point the PBL depth is initialized to some small value so that the entire PBL is contained within the lowest GCM layer. Over time, the PBL may deepen until at some instant its depth is the same as the depth of the lowest GCM layer. We then require that the bulk variables of the PBL agree with the corresponding prognostic variables for the lowest GCM layer, but there is no guarantee that this requirement will be even approximately satisfied.

A solution to this problem was proposed by Randall (1976). Briefly, the idea is to predict the differences between the properties of the PBL and those of the free atmosphere above, rather than to predict the bulk properties of the PBL directly. Randall (1976) further showed that this scheme can be implemented in such a way that the bulk equations (2.2-2.5) are exactly satisfied;

the scheme was implemented in the UCLA GCM by Randall (1976). A modified version of this model has been adopted by the U.S. Navy for operational weather prediction (Rosmond, 1981). Encouraging results obtained with the model have been discussed by Randall (1976) and also by Mechoso et al. (1979), Payne (1980), and Rosmond (1981). However, the approach is very complicated in practice, largely because the GCM layer which contains the PBL top can change from one grid point to the next, and from one time-step to the next. As a result, we have decided not to pursue the method any further at this time.

This chain of reasoning and experience led to the decision, in 1977, to implement the generalized sigma coordinate system described by Suarez and Arakawa (1979). The major advantage of this approach is that the PBL always and everywhere consists of exactly the bottom layer of the GCM. Fig. 6 illustrates the coordinate system, which is defined formally as follows: Let p be the pressure; p_T, the pressure at the top of the model atmosphere, taken as constant; p_B the pressure at the PBL top; p_S the pressure at the earth's surface; and p_I a constant pressure between p_T and a realistic lower bound of p_B (see Fig. 6). Then σ is given by

$$\sigma = \begin{cases} \dfrac{p-p_I}{p_I-p_T} & \text{for} \quad p_T \le p \le p_I, \\ \dfrac{p-p_I}{p_B-p_T} & \text{for} \quad p_T \le p \le p_B, \\ \dfrac{p-p_B}{p_S-p_B} + 1 & \text{for} \quad p_B \le p \le p_S, \end{cases} \tag{6.1}$$

With π defined by

$$\pi = \begin{cases} \pi_K = p_I - p_T & \text{for} \quad -1 \le \sigma < 0, \\ \pi_L = p_B - p_I & \text{for} \quad 0 < \sigma < 1, \\ \pi_M = p_S - p_B & \text{for} \quad 1 < \sigma \le 2, \end{cases} \tag{6.2}$$

the pressure p may be written as

$$p = \begin{cases} p_I + \sigma\pi & \text{for} \quad -1 \leq \sigma < 1, \\ p_B + (\sigma - 1)\pi & \text{for} \quad 1 \leq \sigma < 2. \end{cases} \tag{6.3}$$

The surface $\sigma = 1$ is by definition the PBL top; it is a material surface in the absence of turbulent entrainment (or detrainment) and the loss of turbulent boundary layer air into cumulus clouds with their base at the PBL top.

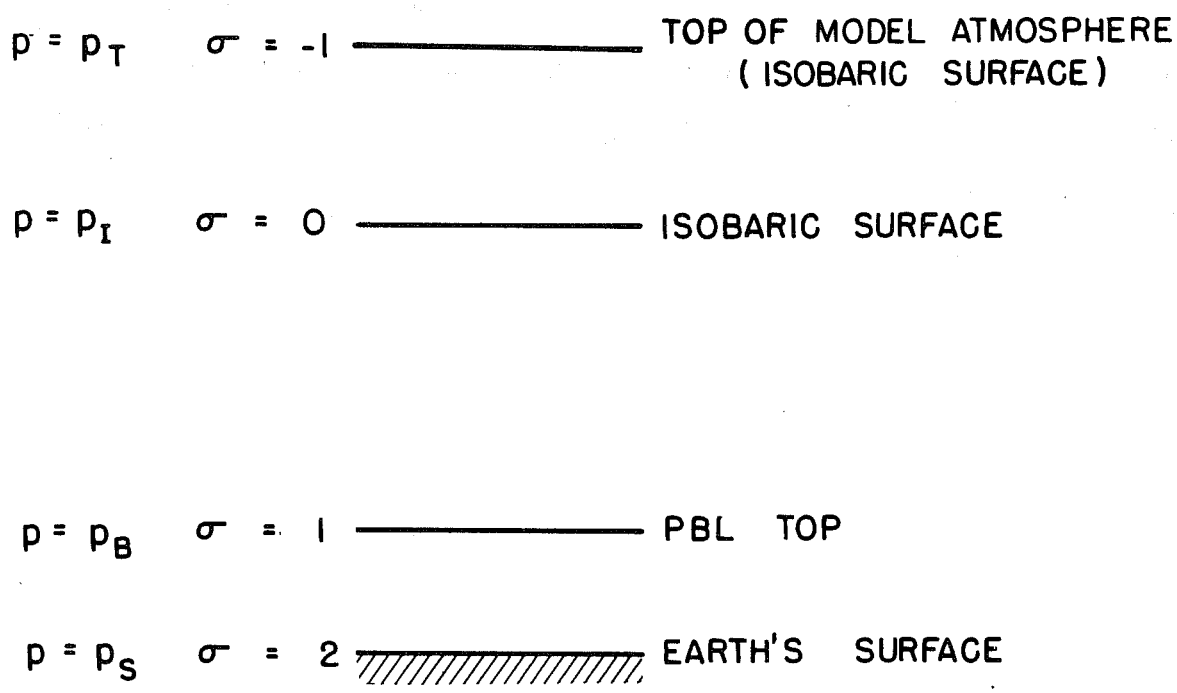

Figure 6. The generalized σ-coordinate system of the UCLA GCM.

6.2 Entrainment

When the interface between a turbulent atmospheric layer and a quiet layer is not simply advected by the mean circulation, but moves progressively into the quiet layer, "entrainment" is said to occur. The entrained air must be supplied with turbulence kinetic energy (TKE), and whenever entrainment occurs across a gravitationally stable interface additional TKE is needed to do work against the stratification. For these reasons, entrainment has often been studied in terms of the conservation of TKE.

The conservation of TKE, as expressed by (2.6), can be written as

$$\frac{1}{g}\mathcal{A} - M_{B+}\, e_{cu,B+} = (B + S) - \frac{1}{g}\int \delta p_M\, D_M\, , \tag{6.4}$$

where

$$\mathcal{A} \equiv \frac{\partial}{\partial t}(e_M \delta p_M) + \nabla \cdot (\underset{\sim}{V}_M e_M \delta p_M) \tag{6.5}$$

represents the rate of <u>storage</u> of TKE in the column, which will be shown to be important during episodes of rapid PBL deepening and shallowing. The buoyancy term of (6.4) includes the rate at which buoyant convection generates TKE, and also the rate at which work must be done to force entrainment against a stable stratification. To expose this negative buoyant production, we write (following Randall, 1980b)

$$B + S = P - N, \tag{6.6}$$

where

$$P = S + \kappa \delta p_M (\lambda F_{sv}/p)_M \tag{6.7}$$

$$N = \kappa \delta p_M [(1 - \lambda) F_{sv}/p]_M \tag{6.8}$$

and

$$\lambda(p) = \begin{cases} 1, & F_{sv}(p) \geq 0 \\ 0, & F_{sv}(p) < 0. \end{cases} \tag{6.9}$$

The positive part of the buoyant production rate is included in P, while the negative part is included in N. It is assumed in this paper that shear production does not contribute to N, although there is some evidence (e.g., Pennell and LeMone, 1974) that this may be an oversimplification.

Under most conditions, the storage term of (6.4) is quite negligible. Kim (1976) suggested that during rapid deepening and shallowing of the ocean mixed

layer the rate of change of the TKE content of the layer is mainly due to the change of the layer depth, rather than the energy density. This implies that

$$\delta = gEe_M \quad , \tag{6.10}$$

and this assumption has been adopted in the UCLA parameterization. Randall (1982) discusses this assumption and its interpretation in some detail. Under such conditions, the rate of change of $e_M \, \delta p_M$, i.e., the change in the TKE content of the layer, is mainly due to the rate of change of δp_M, rather than a decrease in in e_M. A similar assumption was made by Zilitinkevich (1975).

Now define a turbulence velocity scale σ by

$$D_M \equiv \sigma^3 / \delta z_M, \tag{6.11}$$

where δz_M is the PBL depth. Assume that

$$e_M = a_1 \sigma^2, \tag{6.12}$$

where a_1 is a dimensionless constant.

Using (6.6), (6.10), and (6.12), we can rewrite (6.4) as

$$E a_1 \sigma^2 = (P - N) - \beta_M \sigma^3 \quad . \tag{6.13}$$

If P and N can be expressed in terms of E, we can use (6.13) to determine E. But a necessary preliminary step is the prescription of σ .

In nature, P is only modestly larger than $\beta_M \sigma^3$; the terms on the right-hand side of (6.13) tend to cancel, and the left-hand side is their relatively small difference. During deepening (E>0), $Ea_1 \sigma^2$ and N are individually small, and both positive, but their ratio is highly variable. When the PBL deepens through a stable layer entrainment is slow, and $Ea_1 \sigma^2$ is negligible in comparison with N. This most common mode of deepening for the clear convective PBL can be called "buoyancy-limited" entrainment. But when the free atmosphere is weakly or neutrally stratified, entrainment is rapid, and $Ea_1 \sigma^2$ can be much greater than N. The entrainment rate is then "storage-limited." Negative

buoyant production and storage can thus be viewed as two sinks of TKE, competing for the excess of positive production over dissipation. These considerations motivate us to assume that

$$\frac{E a_1 \sigma^2 + N}{(1 - a_2) P} = 1 \qquad (6.14)$$

where a_2 is a constant. The way in which the available gross production is partitioned between storage and negative production is determined by the structure of the free atmosphere into which the PBL grows.

Comparison of (6.13) and (6.14) shows that

$$\int_M \sigma^3 = a_2 P, \qquad (6.15)$$

i.e., the dissipation rate is determined by the total gross production rate P. This is an alternative interpretation of our closure assumption. Because P is defined in such a way that it can never be negative, (6.15) shows that σ can never be negative, and so (6.11) guarantees that the dissipation can never be negative. For the clear unstable PBL, neglecting shear production, σ is approximately proportional to the convective velocity scale of Deardorff (1970), and Tennekes (1970), which is based on the surface buoyant production rate. But because P includes an integral over all regions of positive production throughout the PBL, it also properly reflects buoyant production in the elevated cloud layer of a cloud-topped PBL (Deardorff, 1976; Randall, 1980b). For the neutral or stable PBL σ reduces to a mechanical velocity scale (essentially u_*, the surface friction velocity).

In case storage is negligible, (6.14) reduces to

$$N/P = 1 - a_2, \qquad (6.16)$$

which is the closure assumption of Kraus and Schaller (1978) and Randall (1980b).

For sufficiently large N/P, the storage rate must become negative; the PBL "shallows," and the storage and negative production rates tend to cancel.

Under most conditions, B, S, P and N depend on E, because of the effects of entrainment on the turbulence flux profiles. Deardorff (1973; 1974 a,b) and

others have pointed out that entrainment can strongly influence the flux profiles in the upper PBL, particularly when the PBL top is marked by sharp gradients of potential temperature, moisture, and momentum. Following Randall (1982a), we assume that

$$B = B_0 + B_1 E \quad , \tag{6.17}$$

and

$$S = S_0 + S_1 E \quad , \tag{6.18}$$

where B_0, B_1, S_0, and S_1 are independent of E. These relations can be shown to hold for both clear and stratocumulus-topped mixed layers (Randall, 1982), and we assume that they hold for the stable PBL as well. In addition, we assume that

$$B_1 \leq 0 \quad , \tag{6.19}$$

$$\partial (P - S) / \partial E \leq 0 \quad , \tag{6.20}$$

$$S_0 \geq 0 \quad , \tag{6.21}$$

$$S_1 \geq 0 \quad . \tag{6.22}$$

These inequalities are very useful in the numerical solution of (6.13-14), as discussed by Randall (1982).

The B_1 term of (6.17) can represent the reduction in buoyancy flux due to the entrainment of warm air. The S_1 term of (6.18) can represent the mechanical generation of TKE through erosion of the nocturnal jet (Blackadar, 1957).

For both clear and cloud-topped mixed layers, the forms of B_0, B_1, S_0, and S_1, can be determined. In particular, B_1 and S_1 can be shown to depend on the "jumps" in temperature, mixing ratio, and wind speed at the PBL top. In the UCLA GCM, the values of these jumps are determined by extrapolating from above for the properties at the top of the PBL, then subtracting away the bulk properties.

The top of the stable PBL is not normally marked by jumps; vertical derivatives in the PBL interior are usually at least as strong as those in the air

above. Although the idealized mixed layer models are not applicable to the stable PBL, entrainment can still influence the flux profiles and the TKE production rates. Since entrainment will carry warm air down into the stable PBL, we expect (6.19) to hold, and we assume that (6.17-6.18) and (6.20-6.22) hold as well, with B_0 B_1, S_0, and S_1 independent of E. Moreover, for the stable PBL we determine B_0, B_1, S_0, and S_1, in the same way as for the unstable PBL.

There can be little doubt that this approach does not allow a highly accurate determination of the bulk properties of the stable PBL, or of the associated surface fluxes. However, the surface fluxes of the stable PBL are generally so weak that large fractional error is of little consequence to the large-scale circulation. Similarly, the stable PBL is generally so shallow that a large fractional error in the sunrise PBL depth leads only to minor errors in the depth of the convectively active daytime PBL to follow. From the point of view of the large-scale circulation, it is important that turbulent transfer in the stable PBL is very weak, but the exact intensity of the transfer does not matter much. Of course, for regional air quality modeling and other mesoscale applications, the structure of the stable PBL must be predicted accurately. Bulk models of the stable PBL such as that developed by Nieuwstadt and Tennekes (1981) are well-suited for those applications.

6.3 Diurnal Cycles of the Clear Continental PBL

Now consider a sequence of special cases of entrainment and shallowing, representing a chronological sequence for a typical diurnal cycle of the fair-weather continental PBL. This cycle consists of rapid morning deepening, more gradual afternoon deepening, a sudden shallowing in the early evening, and finally slow deepening through the night.

a) Free entrainment. When the PBL deepens through an isentropic layer, entrainment is rapid and storage-limited. Randall (1982a) shows that, for $B_1=S_1=0$ and $B_0/S_0>>1$,

$$E/(\rho_M w_*) = 2^{-1/3} (1 - a_2) a_2^{-2/3} / a_1 \equiv c_1 \qquad (6.23)$$

where

$$w_* \equiv \left[g \kappa (F_{sv})_S \, \S z_M / \rho_S \right]^{1/3} \qquad (6.24)$$

is the convective velocity scale of Deardorff (1970) and Tennekes (1970). Zilitinkevich (1975) obtained (6.25) theoretically; Deardorff's (1974a) numerical simulation also supports (6.25), with c_1=0.2.

For the freely-entraining neutral (B=0) PBL, we may assume that $P \sim \rho_M u_*^3$, where u_* is the surface friction velocity. It follows that $E \sim \rho_M u_*$, which was previously obtained by Lundgren and Wang (1973), and Zilitinkevich (1975). Here the proportionality factor involves not only a_1 and a_2, but also the ratio of P to $\rho_M u_*^3$. This particular mode of entrainment occurs only infrequently in nature, although it can be produced in the laboratory.

b) Forced entrainment. Within the familiar inversion-capped clear convective mixed layer, F_{sv} decreases linearly with height from positive values near the the surface to negative values near the PBL top. For a sufficiently strong inversion, the entrainment rate will be buoyancy-limited, so that (6.16) will hold. It can be shown that this is equivalent to

$$- (F_{sv})_B / (F_{sv})_S = \sqrt{1 - a_2} \equiv c_2 \, , \qquad (6.25)$$

i.e., the ratio of $(F_{sv})_B$ to $(F_{sv})_S$ approaches a characteristic constant as storage becomes negligible. This relation has been discussed by many authors, beginning with Ball (1960), who took c_2 = 1. Observations and numerical studies summarized by Stull (1976) suggest that c_2=0.2. For c_1=c_2=0.2, we find a_2=0.960 and a_1=0.163. These values are currently used in the UCLA GCM.

c) Shallowing. Near sunset over land, a dramatic change in the PBL structure characteristically occurs, as the ground cools and B goes from positive to negative values (e.g., Carson, 1973; Kaimal et al., 1976; Mahrt, 1981). The turbulence of the deep PBL, produced by mid-day convection, can no longer be maintained by the weak mechanical production near the surface, which must combat an increasingly stable stratification. The PBL then reorganizes itself into a shallow turbulent layer (Businger, 1973), which slowly deepens through the

following night. In the past, some meteorologists (Deardorff, 1972; Randall, 1976) have modelled this shallowing as an instantaneous transition, which occurs when some criterion is satisfied. Criteria for transition and the depth of the PBL after transition have been arbitrarily specified by these authors. Other meteorologists have introduced ad hoc prescriptions to produce a continuous (though rapid) shallowing. The oceanographers, on the other hand, have developed theories of entrainment which explain shallowing in a natural way (Kim, 1976). Because our methods are similar to the oceanographers', our equations also provide a natural explanation of shallowing.

Inspection of (6.13) shows that the sign of E agrees with the sign of the excess of net production over dissipation. When the net production becomes less than the dissipation, E becomes negative, and large negative values can occur. The storage term of (6.13) then becomes negative and large, so that the assumption that a_1 is constant is crucial.

We assume that, whenever E<0, the turbulent fluxes are parametrically independent of E, so that B_1 and S_1 are zero. The reason is that since during shallowing the PBL turbulence is not actively growing into the free atmosphere, but is passively withdrawing from it as a result of dissipation, the rate at which the PBL turbulence retreats cannot be significantly influenced by the free atmosphere above.

Positive production is entirely due to shear, from which it follows that

$$E = \left[B_0 + (1-a_2)S_0 \right] / \left[a_1 (a_2 S_0 / \sigma_M)^{2/3} \right] . \qquad (6.26)$$

For $|B_0| >> (1-a_2)\ S_0$, i.e. strong negative production, we can show that

$$gE / \delta p_M = -gB / (e_M \delta p_M), \qquad (6.27)$$

which means that the time scale for PBL shallowing agrees with the time scale for the destruction of the PBL's TKE content by negative production. For $N / \delta p_M = 3 \times 10^{-3} W\ m^{-2}\ hPa^{-1}$, $g = 9.81\ m\ s^{-2}$, and $a_1 \sigma^2 = 1\ m^2\ s^{-2}$, this time scale is about 0.9 hr, in qualitative agreement with observations of rapid shallowing (e.g., Kaimal et al., 1976).

d) The stable PBL. As a result of radiative cooling at and near the ground, the buoyancy flux is downward at all levels in the nocturnal PBL over land; positive TKE production is entirely due to shear. We therefore have

$$N = -B, \tag{6.28}$$

and

$$P = S. \tag{6.29}$$

Since the stable PBL deepens very slowly, storage is negligible. Then we find that

$$-B/S = 1-a_2 \; ; \tag{6.30}$$

the PBL Richardson number (-B/S) is thus predicted to assume a constant value. We can also show that

$$E = \frac{-[B_0 + (1 - a_2) S_0]}{B_1 + (1 - a_2) S_1} . \tag{6.31}$$

Kato and Phillips (1969) studied the deepening of a mixed layer produced by the application of a surface stress to water in a tank. The stratification was initially stable throughout, but quickly became neutral near the surface as a mixed layer formed and eroded into the quiet water below. Since no surface heating was applied, negative production was solely due to the entrainment of dense water into the mixed layer. In the PBL, this would correspond to

$$N = -B_1 E = 1/2 \left(g \frac{\Delta s_v}{c_p T_s} \delta z_M \right) E. \tag{6.32}$$

If the gross production rate is determined by the surface stress, then we have

$$P = S = S_o = \rho_s u_*^3 / c_u, \tag{6.33}$$

where c_u is a drag coefficient. Substitution of (6.32) and (6.33) into (6.28) yields

$$E = 2 \left(\frac{1-a_2}{c_u} \right) \frac{\rho_s u_*^3}{g \frac{\Delta s_v}{c_p T_s} \delta z_M} . \tag{6.34}$$

This agrees with the form of E suggested by Kato and Phillips, on the basis

of their experiments. In order to match their expression, we need $2(1-a_2)/c_u=2.5$; choice of a_2 is not enough. For $a_2 = 0.96$, c_u is predicted to have the reasonable value 3.2×10^{-2}.

Further discussion of the stable PBL is given by Randall (1982).

6.4 The Stratocumulus-Topped PBL

As discussed by Randall (1980b), in a stratocumulus-topped PBL buoyant production can occur in the cloud layer, the subcloud layer, or both. Radiative cooling near cloud top drives convection, which mixes the layer. Of course, shear production can also be important under some conditions. Simulations with one-dimensional mixed layer models, using the entrainment theory described in the preceding section, confirm that stratocumulus layers will form for sea surface temperatures and large-scale divergences characteristic of the observed marine subtropical stratocumulus regimes.

An interesting moist instability tends to limit the extent of these regimes. As dicussed by Randall (1980a), if the inversion overlying the PBL is not sufficiently strong, entrained parcels will be so strongly cooled by the evaporation of cloud droplets that they will sink unstably as penetrative downdrafts, thus tending to destroy the cloud. The observed inversions are weaker near the equatorward edges of the marine subtropical stratocumulus regimes, suggesting that this instability triggers the transition from stratocumulus to cumulus convection in the trades.

Even when the inversion is strong enough to allow a stable stratus layer, cloud-top evaporation tends to favor large rates of entrainment. For this reason, cloud-topped mixed layers can attain depths on the order of 1 km, even in the face of strong subsidence. Intense cloud-top radiative cooling and cold sea surface temperatures allow the upper part of the PBL to remain saturated even though dry air is being vigorously introduced from above by entrainment.

In the UCLA GCM, the predicted temperature and moisture of the PBL are used to determine the thickness of the saturated layer near the PBL top, where it

occurs. If a stratus layer is present, it is taken into account in determining the entrainment rate, following the methods of Randall (1980b). The radiation parameterization also recognizes the existence of the stratus deck. If the PBL stratus layer is found to be unstable, according to the criterion developed by Randall (1980a), additional entrainment is assumed to occur until the layer becomes stable or is evaporated.

7. RESULTS FROM THE UCLA GCM

We present here some results from a July simulation, initialized from an earlier model run, in which the surface wetness is fixed according to the climatological data of Mintz and Serafini (1981).

Fig. 7 shows the global distribution of PBL depth, averaged over July. The largest time-average values are around 80 mb, and are found over the mid-latitude oceans. Over land, the shallowness of the nocturnal PBL holds the time-averaged depth below 40 mb at most points. In the tropics, strong cumulus subsidence prevents the PBL from becoming very deep.

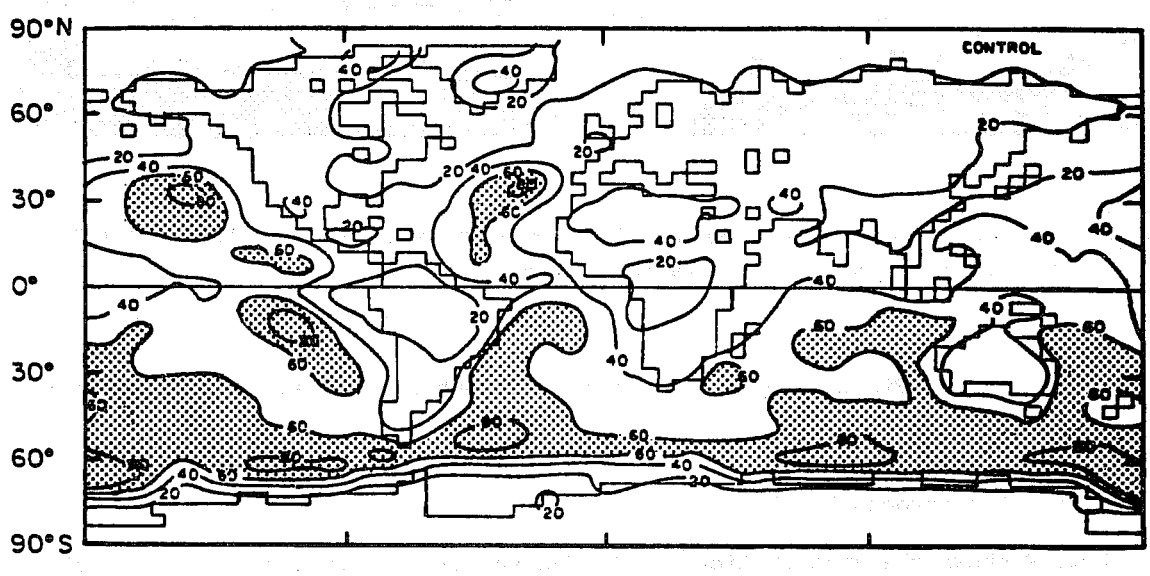

Figure 7. The July mean PBL depth (mb) as simulated by the UCLA GCM. Values greater than 60 mb are shaded.

The July-mean frequency of PBL stratus clouds is shown in Fig. 8. The maxima off the west coasts of North America, South America, and South Africa are correctly located, although their magnitudes are weaker than observed. Weak maxima are also correctly located north of the GATE area, and off the west coast of Australia. The observed Arctic Ocean maximum is not obtained, although the simulation shows a tendency to increased stratus incidence in high northern latitudes. Generally, the global cloudiness pattern simulated by the UCLA model is much more realistic than that simulated by the GLAS model.

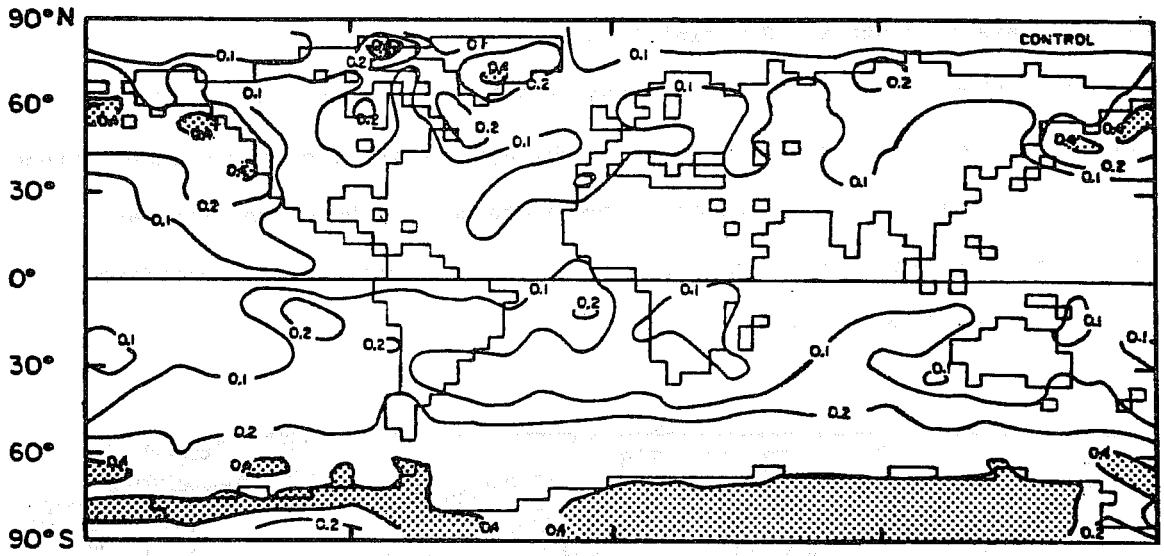

Figure 8. The July mean PBL stratus incidence, as simulated by the UCLA GCM. Values greater than 0.4 are shaded.

Comparison of Figs. 7 and 8 shows that each subtropical stratus frequency maximum is near a maximum in the PBL depth. This is due to rapid entrainment at the top of stratocumulus layers.

Fig. 9 shows the distributions of PBL depth, stratus incidence, and cumulus mass flux off the coast of California. From northeast to southwest, the PBL depth increases, and the stratus regime gives way to a cumulus regime. This is in agreement with the observations of Neiburger (1960; also see Randall, 1980a).

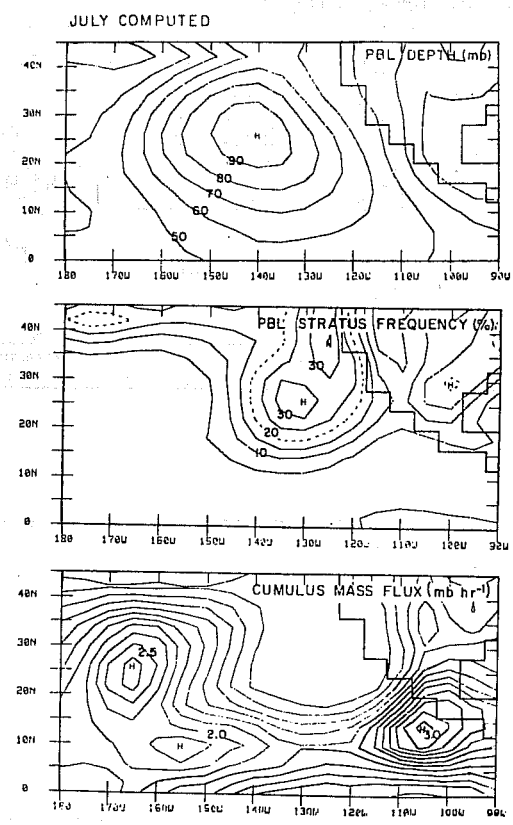

Figure 9. The July mean distributions of PBL depth, stratus incidence, and cloud-base cumulus mass flux, as simulated by the UCLA GCM.

Fig. 11 shows the time variation of the PBL depth, for a nine-day period, over three land points and three ocean points. The locations of the six selected grid points are shown in Fig. 10. The diurnal cycle is prominent for Kansas, and especially for North Africa, where there is little evaporation and the diurnal swing of the ground temperature is therefore very strong. During the North African day, the PBL depth reaches an imposed upper limit of about 130 mb, while at night it diminishes to its imposed lower limit of 10 mb. Over Antarctica, the depth never reaches 50 mb during the nine days shown, and the diurnal cycle is predictably absent during the Antarctic night.

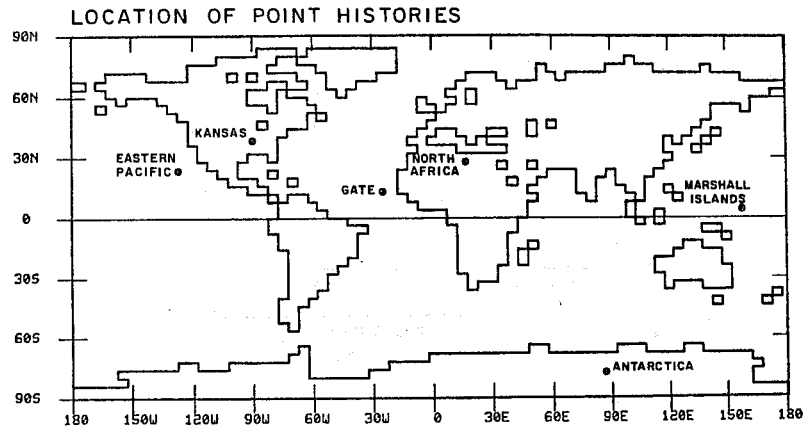

Figure 10. Locations of the six grid points for which nine-day histories are shown in Figs. 11-13.

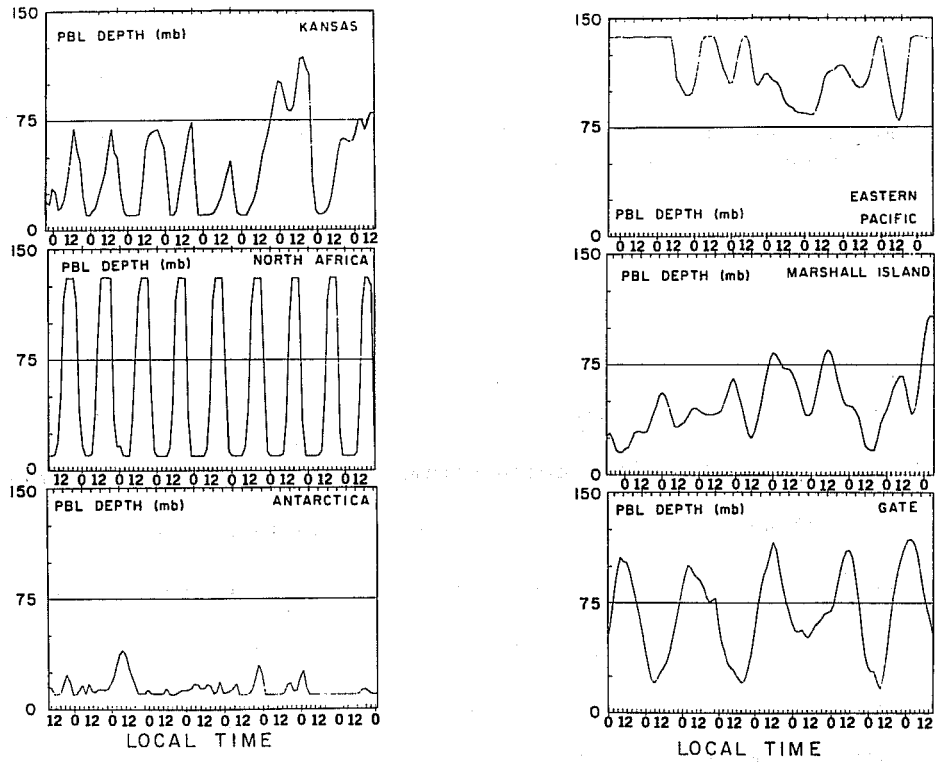

Figure 11. A nine-day history of the PBL depth, for each of the six selected grid points shown in Fig. 10.

Of the three ocean points selected, the greatest PBL depth is found in the Eastern Pacific, where the PBL stratus regime occurs. At this Eastern Pacific point, the PBL depth is never less than 75 mb. There is no evidence of a diurnal cycle. At the Marshall Islands point, the PBL depth varies considerably with time, mainly in relation to the variations of the cumulus mass flux (not shown). There is some tendency for a maximum depth at local midnight, and a minimum at local noon. At the GATE point there is evidence of a remarkable oscillation with a period of about two days.

Comparison of these six histories gives some idea of the variety of PBL regimes that the model is capable of simulating.

Finally, Fig. 12 shows in more detail the evolution of the Kansas PBL over the nine-day period. Intermittent PBL stratus formation modulates the entrainment rate and the ground temperature.

The PBL results shown here are only a small sample of those generated by the UCLA model. Much more can be said about the interaction of the PBL with cumulus convection, the behavior of the PBL in particular synoptic situations, and the role of the layer-cloud instability in limiting the extent of PBL stratocumulus regimes. These and other topics will be discussed elsewhere (Suarez, et al., 1982).

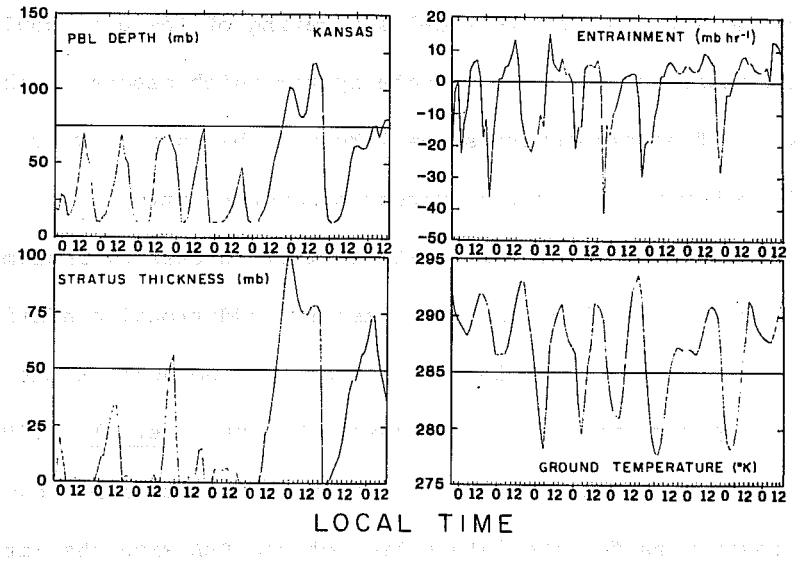

Figure 12. Nine-day histories of the PBL depth, entrainment mass flux, stratus thickness, and ground temperature, for the Kansas grid point.

8. FINAL REMARKS

A simple revision of the surface flux parameterization produced a marked improvement in the sea level pressure pattern simulated by the GLAS GCM. But the model continues to produce excessive low-level cloudiness, leading to an unrealistic planetary albedo, and it fails to simulate some of the most conspicuous regional cloud patterns observed in nature.

These deficiencies are largely remedied in the UCLA model, as a consequence of the model's explicit coupling of the PBL parameterization with the parameterizations of cumulus and stratus clouds. This model simulates many observed PBL climate statistics, such as the distribution of the PBL depth, the incidence of PBL stratocumulus clouds, and the response of the PBL to cumulus convection. These are important aspects of the global climate. Moreover,the ground-wetness sensitivity study of Suarez and Arakawa (1982; see also Mintz, 1982) demonstrates that the response of the simulated climate to changes in external forcing is significantly influenced by the PBL parameterization.

The generalized sigma coordinate system seems to be a key to the success of the UCLA parameterization. As described above, alternative possibilities were explored for incorporating the variable-depth PBL into the GCM, but each had serious drawbacks. In the future, additional vertical resolution could be provided within the PBL, and the vertical staggering of the grid could be altered. Nevertheless, use of a coordinate system which separates the PBL turbulence from the free atmosphere seems likely to be an idea which will outlive many of the other facets of the current parameterization.

Given the generalized sigma coordinate system, successful implementation of the parameterization requires that at least two additional conditions be met. First, the diurnal cycle of solar insolation must be included in the model. As emphasized in this paper, and also as discussed by Suarez et al. (1982) and Suarez and Arakawa (1982), the diurnal variation of the PBL depth over land has profound consequences for the interaction of the PBL with the large-scale

circulations. The observed diurnal variability of convective precipitation over land has been documented by Wallace (1975) and others, and is undoubtedly associated with the diurnal variation of PBL processes. Gray and Jacobsen (1977) have pointed out significant observed diurnal variations in convective precipitation over the tropical oceans. The UCLA parameterization has been designed to allow simulation of such diurnal variations, and it would be wasted in a model without a diurnal insolation cycle.

Finally, it is essential that the cumulus parameterization predict the cumulus mass flux at the PBL top. As discussed by Randall (1976) and Suarez et al. (1982), the PBL depth in the tropics is determined by a balance between the tendency of the PBL to deepen through turbulent entrainment and the tendency of cumulus clouds to remove mass from the PBL. If the cumulus mass flux were to be neglected, entrainment would lead to an unrealistically deep PBL over large portions of the tropics; the simulation would be ruined.

9. ACKNOWLEDGEMENTS

In collaboration with the author, Professors Akio Arakawa and Max Suarez of UCLA have made essential contributions to the development and implementation of the PBL parameterization in the UCLA model. They kindly made available the UCLA GCM results presented in this paper.

Professor Yale Mintz carried out a very helpful review of the manuscript.

A portion of this material is based upon work supported jointly at UCLA by the National Science Foundation and the National Oceanic and Atmospheric Administration under Grant Number ATM-8108798. Computer time for integration of the UCLA model was provided by Scientific Computing Division, National Center for Atmospheric Research.

10. REFERENCES

Arakawa, A., 1972: Design of the UCLA general circulation model. Numerical Simulation of Weather and Climate, Technical Report No. 7, Dept. Meteorology, University of California, Los Angeles, 116 pp.

Arakawa, A., and W. H. Schubert, 1974: Interaction of a cumulus cloud ensemble with the large-scale environment, Part I. J. Atmos. Sci., 31, 674-701.

Ball, F. K., 1960: Control of inversion height by surface heating. Quar. J. Roy. Meteor. Soc., 86, 483-494.

Blackadar, A. K., 1957: Boundary layer wind maxima and their significance for the growth of nocturnal inversions. Bull. Amer. Meteor. Soc., 38, 283-290.

Bunker, A. F., B. Haurwitz, J. S. Malkus and H. Stommel, 1949: Vertical distribution of temperature and humidity over the Carribean Sea. Papers Phys. Oceanogr. Meteor., 11, 82 pp.

Businger, J. A., J. C. Wyngaard, Y. Izumi, and E. F. Bradley, 1971: Flux-profile relationships in the atmospheric surface layer. J. Atmos. Sci., 28, 181-189.

Businger, J. A., 1973: Turbulent transfer in the atmospheric surface layer. Workshop on Micrometeorology, D. A. Haugen, Ed., Amer. Meteor. Soc., Boston, 67-100.

Carson, D. J., 1973: The development of a dry inversion-capped convectively unstable boundary layer. Quar. J. Roy. Meteor. Soc., 99, 450-467.

Charney, J. G., and A. Eliassen 1949: A numerical method for predicting the perturbations of the middle latitude westerlies. Tellus, 1, 38-54.

Deardorff, J. W., 1970: Convective velocity and temperature scales for the unstable planetary boundary layer and for Rayleigh convection. J. Atmos. Sci., 27, 1211-1213.

Deardorff, J. W., 1972: Parameterization of the planetary boundary layer for use in general circulation models. Mon. Wea. Rev., 100, 93-106.

Deardorff, J. W., 1973: An explanation of anomalously large Reynolds stresses within the convective planetary boundary layer. J. Atmos. Sci., 30, 1070-1076.

Deardorff, J. W., 1974a: Three-dimensional numerical study of the height and mean structure of a heated planetary boundary layer. Boundary Layer Meteor., 7, 81-106.

Deardorff, J. W., 1974b: Three-dimensional numerical study of turbulence in an entraining mixed layer. Boundary Layer Meteor., 7, 199-266.

Deardorff, J. W., 1976: On the entrainment rate of a stratucumulus-topped mixed layer. Quar. J. Roy. Meteor. Soc., 102, 563-582.

Gray, W. M., and R. W. Jacobsen, Jr., 1977: Diurnal variation of oceanic deep cumulus convection. Mon. Wea. Rev., 105, 1171-1188.

Halem, M., J. Shukla, Y. Mintz, and M. L. Wu, R. Godbole, G. Herman, and Y. Sud, 1979: Comparisons of observed seasonal climate features with a winter and summer numerical simulation produced with the GLAS General Circulation Model. GARP Publ. Series No. 22, 207-253, WMO, Geneva, Switzerland.

Helfand, H. M., 1979: The effect of cumulus friction on the simulation of the January Hadley circulation by the GLAS model of the general circulation. J. Atmos. Sci., 36, 1827-1843.

Herman, G., and R. Goody, 1976: Formation and persistence of summertime artic stratus clouds. J. Atmos. Sci., 33, 1537-1553.

Kaimal, J. C., J. C. Wyngaard, D. A. Haugen, O. R. Cote, Y. Izmuzi, S. J. Caughey, and C. J. Readings, 1976: Turbulence structure in the convective boundary layer. J. Atmos. Sci., 33, 2152-2169.

Kantha, L. H., O. M. Phillips, and R. S. Azad, 1977: On turbulent entrainment at a stable density interface. J. Fluid Mech., 79, 753-768.

Kato, H., and O. M. Phillips, 1969: On the penetration of a turbulent layer into stratified fluid. J. Fluid Mech., 37, 643-655.

Kim, J.-W., 1976: A generalized bulk model of the oceanic mixed layer. J. Phys. Ocean., 6, 686-695.

Lilly, D. K., 1968: Models of cloud-topped mixed layers under a strong inversion. Quar. J. Roy. Meteor. Soc., 95, 292-309.

Lord, S. J., and A. Arakawa, 1980: Interaction of a cumulus cloud ensemble with the large-scale environment, Part II. J. Atmos. Sci., 37, 2677-2792.

Lord, S. J., 1982: Interaction of a cumulus cloud ensemble with the large-scale environment. Part III. Semi-prognostic test of the Arakawa-Schubert cumulus parameterization. J. Atmos. Sci., 39, (to appear).

Lord, S. J., W. C. Chao, and A. Arakawa, 1982: Interaction of a cumulus cloud ensemble with the large-scale environment. Part IV. The discrete model. Submitted to J. Atmos. Sci., 39, (to appear).

Lundgren, T. S., and F. C. Wang, 1973: Eddy viscosity models for free turbulent flows. Phys. Fluids, 16, 174-178.

Mahrt, L., 1981: The early evening boundary layer transition. Quar. J. Roy. Meteor. Soc., 107, 329-343.

Malkus, J. S., 1954: Some results of a trade-cumulus cloud investigation. J. Meteor., 11, 220-237.

Mechoso, C. R., M. J. Suarez, and A. Arakawa, 1979: July simulation by the UCLA general circulation model. Fourth Conference on Numerical Weather Prediction of the Amer. Meteor. Soc., Silver Spring, Maryland, Oct. 29 - Nov. 1, 1979, pp. 282-289.

Mechoso, C. R., M. J. Suarez, K. Yamazaki, J. A. Spahr, and A. Arakawa, 1981: Winter simulation of standing and travelling waves with the UCLA general circulation model. Fifth Conf. on Num. Wea. Pred. of the Amer. Meteor. Soc., Monterey, Calif., November 2-6, pp. 60-67.

Mintz, Y., and Y. Serafini, 1981: Monthly normal global fields of soil moisture and land-surface evapotranspiration. International Symposium on Variations in the Global Water Budget. Oxford, England, August 10-15, 1981. (manuscript in preparation).

Mintz, Y., 1982: The influence of land-surface evapotranspiration on rainfall and circulation: A review of general circulation experiments. In preparation.

Moss, M. R., and S. L. Rosenthal, 1975: On the estimation of planetary boundary layer bariables in mature hurricances. Mon. Wea. Rev., 103, 980-988.

Neiburger, M., 1960: The relation of air mass structure to the field of motion over the Eastern North Pacific Ocean in summer. Tellus, 12, 31-40.

Nieuwstadt, F. T. M., and H. Tennekes, 1981: A rate equation for the nocturnal boundary layer height. J. Atmos. Sci., 38, 1418-1428.

Payne, S. W., 1980: Preliminary results of a comparison of the Navy Northern Hemisphere primitive equation model with the NEPRF/UCLA global forecast system. Eighth Conf. on Forecasting and Analysis of the Amer. Meteor. Soc., Denver, Colorado, June 10-13, 1980, pp. 496-499.

Pennel, W. T., and M. A. LeMone, 1974: An experimental study of turbulence structure in the fair-weather trade wind boundary layer. J. Atmos. Sci., 31, 1308-1323.

Randall, D. A., 1976: The interaction of the planetary boundary layer with large-scale circulations. Ph.D. Thesis, The University of California, Los Angeles, 247 pp.

Randall, D. A., 1980a: Conditional instability of the first kind, upside-down. J. Atmos. Sci., 37, 125-130.

Randall, D. A., 1980b: Entrainment into a stratocumulus layer with distributed radiative cooling. J. Atmos. Sci., 37, 148-159.

Randall, D. A., 1982: A planetary boundary layer parameterization for global atmospheric models. In preparation.

Randall, D. A., and L. Marx, 1982: The GLAS Seasonal Cycle Model. In preparation as a NASA Technical Memorandum.

Riehl, H., and J. S. Malkus, 1958: On the heat balance in the equatorial through zone. Geophysica, 6, 503-537.

Rosmond, T. E., 1981: NOGAPS: Navy operational global atmospheric prediction system. Fifth Conference on Numerical Weather Prediction of the Amer. Meteor. Soc., Monterey, Calif., November 2-6, pp. 74-79.

Shukla, J., D. Straus, D. A. Randall, Y. Sud, and L. Marx, 1982: Winter and summer simulations with the GLAS climate model. In preparation as a NASA Techical Memorandum.

Smagorinski, J., S. Manabe, and J. L. Holloway, Jr., 1965: Numerical results from a nine-level general circulation model of the atmosphere. Mon. Wea. Rev., 93, 727-768.

Somerville, R. C. J., P. H. Stone, M. Halem, J. E. Hansen, J. S. Hogan, L. M. Druyan, G. Russell, A. A. Lacis, W. J. Quirk, and J. Tennenbaum, 1974: The GISS model of the global atmosphere. J. Atmos. Sci., 31, 84-117.

Stull, R. B., 1976: The energetics of entrainment across a density interface. J. Atmos. Sci., 33, 1260-1267.

Suarez, M. J., and A. Arakawa, 1979: Description and preliminary results of the 9-level UCLA general circulation model. The Fourth Conference on Numerical Weather Prediction, October 29 - November 1, 1979, Silver Spring, Maryland, American Meteorological Society, Boston, Mass.

Suarez, M., and A. Arakawa, 1982: Sensitivity of the UCLA general circulation model to changes in ground wetness. In preparation.

Suarez, M., A. Arakawa, and D. Randall, 1982: Simulation of the planetary boundary layer with the UCLA general circulation model. In preparation.

Tennekes, H., 1970: Free convection in the turbulent Ekman layer of the atmosphere. J. Atmos. Sci., 27, 1027-1034.

Wallace, J. M., 1975: Diurnal variations in precipitation and thunderstorm frequency over the coterminous United States. Mon. Wea. Rev., 103, 406-419.

Zilitinkevich, S. S., 1975: Comments on "A model for the dynamics of the inversion above a convective boundary layer." J. Atmos. Sci., 32, 991-992.